Supramolecular organization and siRNA binding of hyaluronic acid-coated lipoplexes for targeted delivery to the CD44 receptor.

Supramolecular Organization and siRNA Binding of Hyaluronic Acid-Coated Lipoplexes for Targeted Delivery to the CD44 Receptor

Thais L. Nascimento[†‡§], Hervé Hillaireau[†‡], Magali Noiray[†‡], Claudie Bourgaux[†‡], Silvia Arpicco[‖], Gérard Pehau-Arnaudet[⊥], Myriam Taverna[†‡], Donato Cosco[#], Nicolas Tsapis[†‡], and Elias Fattal[*†‡]

[†] Faculté de Pharmacie, Institut Galien Paris-Sud. Université Paris-Sud, LabEx LERMIT, 5 rue JB Clément, 92296 Châtenay-Malabry Cedex, France
[‡] CNRS, UMR 8612, 5 rue JB Clément, 92296 Châtenay-Malabry Cedex, France
[§] CAPES Foundation, Ministry of Education of Brazil, Brasília DF 70040-020, Brazil
[‖] Dipartemento di Scienza e Tecnologia del Farmaco, Università degli Studi di Torino, Facoltà di Farmacia, Via Pietro Giuria 9, 10125 Torino, Italy
[⊥] Institut Pasteur, Plate-Forme de Microscopie Ultrastructurale, 25−28 rue du Docteur Roux, 75015 Paris, France
[#] Department of Health Sciences, University "Magna Græcia" of Catanzaro, Campus Universitario "S. Venuta", Viale S. Venuta, Germaneto, I-88100 Catanzaro, Italy

*Tel: +33146835568. Fax: +33146835946. E-mail: elias.fattal@u-psud.fr.

Abstract

The dynamics of the formation of siRNA-lipoplexes coated with hyaluronic acid (HA) and the parameters influencing their supramolecular organization were studied. The insertion of a HA-dioleylphosphatidylethanolamine (DOPE) conjugate in the liposome structure as well as subsequent complexation with siRNA increased the liposome size. Lipoplexes were around 110 nm at high ± charge ratios with a zeta potential around +50 mV and around 230 nm at low ± ratios, with a zeta potential that decreased to negative values, reaching −45 mV. The addition of the conjugate did not compromise siRNA binding to liposomes, although these nucleic acids induced a displacement of part of the HA-DOPE conjugate upon lipoplex formation, as confirmed by capillary electrophoresis. Isothermal titration calorimetry, X-ray diffraction studies, and cryo-TEM microscopy demonstrated that in addition to electrostatic interactions with siRNA a rearrangement of the lipid bilayers takes place, resulting in condensed oligolamellar vesicles. This phenomenon is dependent on the number of siRNA molecules and the degree of modification with HA. Finally, the suitable positioning of HA on the lipoplex surface and its ability to bind specifically to the CD44 receptors in a concentration-dependent manner was demonstrated by surface plasmon resonance analysis.

Introduction

The downregulation of gene expression using small interfering RNA (siRNA) has raised broad interest in medical applications. siRNAs are short double-stranded RNA molecules of 19–21 nucleotides in length that besides being highly efficient and selective offer the possibility of a long-lasting therapeutic effect for gene-related diseases. One of the strands is called the guide, which is complementary to the coding region of the target mRNA, while the other is known as the passenger strand. Once in the cytoplasm, the guide strand binds to the target RNA molecule, which promotes the enzymatic cleavage of the mRNA and prevents the synthesis of the protein of interest. However, these molecules face some impediments to successful application, similarly to other nucleotide-based therapeutics such as plasmid DNA and antisense oligonucleotides.(1) As a result of their small size, they are rapidly eliminated by the kidneys and show circulating half-lives of seconds to minutes.(2) They are also susceptible to degradation by nucleases in the plasma. Within the tissues, they do not cross cell membranes readily because of their negative charge, hydrophilicity, and molecular size. Also, siRNAs are taken up by most mammalian cells in a way that does not preserve their activity.(3) Therefore, the future of this therapeutic approach heavily depends on the development of delivery systems able to carry these molecules from their administration site to their intracellular pharmacological target.(4)

Complexes formed by electrostatic interactions between cationic liposomes and siRNA, called lipoplexes, are considered to be the most suitable carriers for the intracellular delivery of nucleic acids, particularly for siRNA.(5, 6) In addition, they are versatile systems whose surfaces can be modified to increase their circulation time and improve their interaction with the target.(7) One of the key factors influencing siRNA delivery is the macromolecular shape of the lipoplex.(8, 9) Their final structure has a significant impact on particle stability, interaction with biological components, cytotoxicity,(9, 10) and intracellular trafficking(11, 12) and will therefore determine their efficiency in vitro and in vivo.(13) It is therefore important to consider an accurate and detailed understanding of lipoplex structure and physicochemical characteristics.

Hyaluronic acid (HA) is a glycosaminoglycan polymer composed of disaccharide units of *N*-acetylglucosamine and d-glucuronic acid linked together through alternating β-1,3 and β-1,4 glycosidic bonds.(14) It is biocompatible, being the major component of the extracellular matrix. The native high-molecular-weight HA is nontoxic and nonimmunogenic.(15) It does not induce an expression of genes involved in proliferation or inflammation(16) and counteracts proangiogenic effects of the HA oligomers.(17, 18) Surface modification of cationic liposomes with high-molecular-weight HA can improve their efficacy by mediating active CD44 targeting in tumors and can also increase their circulation time because of a possible dysopsonization effect due to the hydrophilic coating effect of HA.(19-22)

In this study, we describe the design and physicochemical characterization of novel HA-lipoplexes entrapping siRNA. The lipoplex composition is based on cationic lipid 2-(2,3-didodecyloxypropyl)hydroxyethyl] ammonium bromide (DE), which has shown promising transfection efficiency in different cell lines compared to the cationic lipids currently available on the market.(23) To achieve the targeting of CD44 receptors, lipoplexes were surface-coated using a conjugate of HA and l-α-dioleylphosphatidylethanolamine (DOPE).(24) In previous studies, the modification of lipoplexes with the HA-DOPE conjugate demonstrated increased transfection of CD44-expressing cells using plasmid DNA(18, 25) and siRNA.(24) The supramolecular organization and formation of these lipoplexes, however, remained an open question. Here, a study of the formation of these nanocarriers and the aspects influencing the organization of the lipid bilayers was performed using a combination of dynamic light scattering, capillary electrophoresis, cryo-TEM microscopy, surface plasmon resonance, and small-angle X-ray scattering techniques.

Experimental Section

Materials

Cationic lipid [2-(2,3-didodecyloxypropyl)hydroxyethyl] ammonium bromide (DE) was synthesized as described previously.(23) l-α-Dioleylphosphatidylethanolamine (DOPE) and phosphatidylethanolamine conjugated to rhodamine (PE-rhodamine) were purchased from Avanti Polar Lipids distributed by Sigma-Aldrich (Saint Quentin Fallavier, France). High-molecular-weight HA (sodium salt, 1600 kDa, purity of 95%) was provided by Acros Organics (Geel, Belgium). SiRNA (19 bp) was purchased from Eurogentec (Angers, France) and diluted in RNase-free water before use. The HA-DOPE conjugate was synthesized as described previously.(25) In the following text, water refers to ultrapurified Milli-Q water (Millipore, France) with a resistivity of ≥18 MΩ·cm.

Liposome and Lipoplex Preparation

Liposomes of DOPE/DE in a 1:1 w/w ratio (equivalent to a molar ratio of 0.78:1) were prepared in water by the ethanol injection method.(24, 26) Separate solutions of DE and DOPE, stored in chloroform under nitrogen at −20 °C, were dried under pressure in a rotary evaporator. The dried lipids were then dissolved in absolute ethanol at a concentration of 10 mg/mL. For liposome preparation, 0.06 to 0.9 mL of the ethanolic lipid solution was rapidly injected into RNase-free water under magnetic stirring. HA-liposomes were prepared by diluting an aqueous stock solution of the HA-DOPE conjugate (1 mg/mL) to different concentrations in RNase free water before injection. Each conjugate has 3 μg of DOPE/mg of HA. The HA-DOPE content of liposomes is expressed as the mass ratio of HA-DOPE to other lipids (DE + DOPE) (10% refers to 1:10 w/w). Liposome suspensions were dialyzed against 1 L of Milli-Q water overnight in Spectra/Por CE dialysis tubes with a molecular weight cutoff of 50 kDa (Spectrum Laboratories, Breda, Netherlands) to eliminate ethanol. Lipoplexes were then prepared at different charge ratios (± ratios) by adding 1 volume of the 3 mM liposome suspension to 2 volumes of siRNA solution at different concentrations (0.11, 0.16, 0.22, 0.44, 5.52, 7.36, 11.05, and 22.10 μM for ± ratios of 200, 134, 100, 50, 4, 3, 2, and 1) in an Eppendorf tube and gently homogenizing by pipetting up and down. Suspensions of 15 μL – 2.5 mL of lipoplexes were usually prepared and incubated for 1 h at room temperature before use.

Hydrodynamic Diameter and Zeta Potential Measurements

The mean hydrodynamic diameter, polydispersity index (PdI), and zeta potential were determined with a Zetasizer Nano Zs (Malvern Instruments Ltd., Malvern, U.K.). Before each measurement, liposomes and lipoplexes were diluted in 1 mM NaCl. Measurements were carried out in triplicate at 25 °C for at least three independent preparations.

Colloidal Stability of Lipoplexes in Isotonic Media

Noncoated, 10% HA-liposomes and HA-lipoplexes at various charge ratios were prepared as described above and diluted down to 66 μg/mL of lipids with 0.9% w/v NaCl or 5% w/v glucose. Changes in hydrodynamic diameter upon dilution were monitored at 25 °C. The accuracy of measurements was verified by mixing each suspension thoroughly before each measurement. All experiments were performed at least in duplicate.

Lipoplex siRNA Content

siRNAs were labeled at the 5′-end with γ-^{33}P-ATP (PerkinElmer Life Sciences, Courtaboeuf, France) as catalyzed by T4 polynucleotide kinase (New England Biolabs, Frankfurt am Main, Germany) according to the manufacturer's protocol. Lipoplexes were prepared with radiolabeled siRNA at various ± ratios (2–134) from noncoated or 10% HA-liposomes. Suspensions were placed in the upper chamber of Amicon Ultra 0.5 mL filters (cutoff value 100 kDa; Millipore). After adding 200 μL of RNase-free water, samples were centrifuged (14 000*g*, 30 min, 4 °C). This procedure was repeated five times. Binding efficiencies were determined by comparing the sum of the specific radioactivity

of the washings to the radioactivity of the siRNA solution used for the lipoplex preparation. Experiments were performed in triplicate.

Capillary Electrophoresis

A Beckman P/ACE System 5500 was used with an uncoated fused silica capillary of 57 cm effective length and an internal diameter of 75 μm. Electrophoresis conditions to analyze the HA-DOPE conjugate were derived from Grimshaw et al.(27) for the assay of HA. The capillary was first conditioned by four successive rinsing steps of 5 min each with water, 1 M NaOH, 0.1 M NaOH, and back to water. Before each analysis, the capillary was washed at 20 psi with water for 2 min and 0.1 M NaOH for 3 min and finally equilibrated with the background electrolyte for 5 min. The separation buffer was 65 mM sodium tetraborate containing 20 mM sodium dodecyl sulfate (SDS) at pH 9.0. Sample injection was carried out at 0.5 psi for 5 s. All samples were adjusted to a concentration of 1 mg/mL of HA or HA-DOPE by evaporation under vacuum using an Eppendorf Concentrator at 30 °C. This step was validated after verification by dynamic light scattering that no modification of the diameter and zeta potential occurred during the concentration. The free fraction of conjugate was determined using a HA-DOPE 1 mg/mL solution as an internal standard. Samples containing 1 mg/mL HA-DOPE + HA-DOPE solutions at 0.25, 0.5, 1, and 2.5 mg/mL were analyzed, and the peak areas obtained were used to form calibration curves. The peak areas found by extrapolation of the sample curves to the point [HA-DOPE] = 0 were used in the HA-DOPE calibration curve to determine the free amount of conjugate. The detection wavelength was 200 nm, and the voltage applied was +25 kV. The capillary was maintained at 25 °C during electrophoresis. Experiments were performed at least in duplicate.

Isothermal Titration Calorimetry

The thermodynamics of the interaction between siRNA and the cationic liposomes, coated or not with HA, was evaluated by isothermal titration calorimetry (ITC) (Microcal Inc., USA). Aliquots of 10 μL of aqueous siRNA solution (19.7 μM) placed in a 283 μL syringe were used to titrate the aqueous suspension of liposomes (98 μM total lipids) in the calorimetric sample cell accurately thermostated at 25 °C. The agitation speed was 307 rpm, and the interval between injections was 500 s. The titration background consisted of injecting the siRNA solution in Milli-Q water. The heats of dilution were insignificant compared to the binding interaction heats.

Cryo-transmission Electron Microscopy

HA-liposomes (10%) and HA-lipoplexes containing siRNA at ± ratios of 2 and 134 were observed using cryo-transmission electron microscopy (cryo-TEM). The preparation of liposome samples was performed as follows. A concentrated liposome aqueous suspension (4 μL) was placed on Quantifoil R2/2 grids (Quantifoil, Germany). The samples were cryofixed in liquid ethane (−180 °C) using the Leica EMGP (Leica, Austria). For lipoplex samples, grids were pretreated with 1 mM $CaCl_2$ for 1 min. Grids were transferred using a cryo-holder (626 DH Gatan) for observation on a Tecnai F20 electron microscope (FEI, USA). Images were recorded under low-electron-dose conditions at 200 kV on a Gatan Ultrascan 4000 camera with Digital Micrograph (Gatan, USA) version 1.83.842. Doses were previously quantified using a faraday cup.

Small-Angle X-ray Scattering (SAXS)

Suspensions of liposomes and lipoplexes were loaded into quartz capillaries (diameter 1.5 mm, Glas-Müller, Berlin, Germany). The top of the capillaries was sealed with a drop of paraffin to prevent water evaporation. Small-angle X-ray scattering experiments were performed on the SWING beamline at the SOLEIL synchrotron. The energy was set to 11 keV. The scattering intensity was reported as a function of scattering vector $q = {}^{4\pi}/_{\lambda} \sin\theta$, where 2θ is the scattering angle and λ is the wavelength of the incident beam. Calibration of the q range (0.008–0.4 $Å^{-1}$) was carried out with silver behenate as the standard. Data were collected with a two-dimensional CCD detector. The

acquisition time was 50 s. Intensity values were normalized to account for the beam intensity, acquisition time, and sample transmission. Each scattering pattern was then integrated circularly to yield the intensity as a function of q. The scattering intensity from a capillary filled with water was subtracted from the sample scattering curves.

HA-Lipoplex CD44 Receptor Affinity by Surface Plasmon Resonance Spectroscopy

The interaction of noncoated and HA-lipoplexes with CD44 receptors was monitored by surface plasmon resonance (SPR) spectroscopy using a BIAcore T100 (GE Healthcare Life Sciences, Vélizy, France) instrument. Human recombinant CD44-Fc receptors were immobilized on a carboxymethylated dextran sensor chip (series S CM3, GE Healthcare) using amine coupling. Carboxylic groups were activated by a mixture of EDC/NHS for 7 min at 10 μL/min followed by an injection of 17 μg/mL CD44-Fc in a 10 mM acetate buffer at pH 4.4 for 5 min at 10 μL/min. The remaining groups were blocked by an injection of ethanolamine. A flow channel blocked by ethanolamine was used as a reference surface. The specific interaction of HA-lipoplexes (at concentrations 0.3, 0.6, 1.2, 2.4, and 4.8 μM lipids) with the immobilized CD44-Fc was assessed. All experiments were conducted at a flow rate of 50 μL/min in 150 mM NaCl with a contact time of 360 s. The surface was washed for 640 s and regenerated with a 34 mM octyl-glucoside solution for 30 s at 50 μL/min and 10 mM NaOH for 30 s at 100 μL/min after each sample analysis. Free 1600 kDa HA solution was systematically passed through the channel to verify the integrity of the CD44-Fc receptors. The analyses were performed in triplicate using BIAcore T100 evaluation software, version 2.0.2 (GE Healthcare).

Results and Discussion

In this study, siRNA-loaded lipoplexes coated with hyaluronic acid (HA) were formulated and characterized to investigate their structure and affinity for CD44 receptors, with a view to developing effective gene-silencing nanomedicines targeting this receptor, a key marker of cancer metastasis. We have chosen to coat the lipoplexes with a large-molecular-weight HA since we have already shown that an increased internalization of siRNA binding of these HA-lipoplexes was obtained in CD44-expressing cells.(24) SiRNA HA-lipoplexes were characterized here using a combination of a light-scattering technique, radioactive labeling, diameter and surface charge analyses, capillary electrophoresis, cryo-TEM microscopy, SAXS, and surface plasmon resonance.

To insert HA into the lipoplex structure, a HA-DOPE conjugate was prepared by a condensation reaction between the carboxylic residues of HA and amino groups of DOPE lipids. DOPE within the conjugate was used as a lipid anchor. The absence of free DOPE on the conjugate was confirmed by thin-layer chromatography, and the amount of lipids was quantified as 1.1 ± 0.5% w/w using Stewart assay.(28) Noncoated liposomes obtained by the ethanol injection method were 88 ± 8 nm in size (Figure 1). The effect of HA-DOPE insertion on the diameter and zeta potential was studied by adding 0, 5, 10, and 15% (w/w) conjugate when preparing the liposomes. A gradual increase in diameter with increasing HA-DOPE content was observed (Figure 1), indicating the insertion of HA in the liposome structure. Liposomes with 15% HA-DOPE reached diameters of 142 ± 19 nm, and larger amounts of conjugate resulted in the formation of agglomerates, probably due to a bridging interaction between HA molecules on the lipoplex surface. Noncoated and HA-liposomes maintained their size for at least 4 months when stored at 4 °C. The absence of vesicles or micelles formed by the HA-DOPE conjugate itself was confirmed using light-scattering measurements. Zeta potential values were positive in the range of +55 to +30 mV for liposome preparations due to the presence of amino groups of cationic lipid DE, gradually decreasing with increasing amounts of HA-DOPE conjugate, again confirming the presence of HA on the surface of the particles.

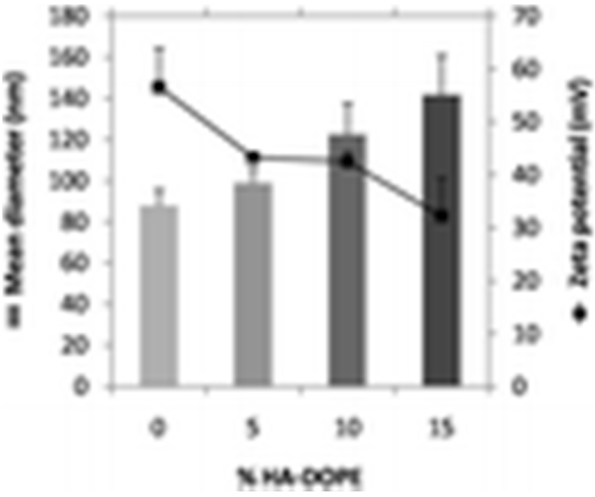

Figure 1. Mean hydrodynamic diameter and zeta potential of cationic liposomes prepared without or with 5, 10, or 15% HA-DOPE (n = 3). Data = mean ± SD.

HA-DOPE (10%) was chosen for the preparation of lipoplexes. This amount was previously shown to be an optimal amount for the transfection of MDA-MB231 and A549 cancer cells expressing CD44.(18, 25) The complexation of liposomes with siRNA at low concentrations (± ratios of 200, 100, and 50) resulted in lipoplexes with diameters comparable to those of liposomes, around 90 nm for the noncoated and 120 nm for the HA-liposomes (Figure 2). When larger amounts of siRNA were complexed (at ratios 4, 3, 2, and 1), the diameters of noncoated and HA-liposome increased to around 140 and 230 nm, respectively (Figure 2). The size distribution in these samples was quite large. The

PdI of HA-liposomes and HA-lipoplexes was, however, below 0.23 for all lipoplex formulations. The zeta potential measurements of lipoplexes clearly confirmed differences in the degree of surface modification. Between ratios of 200 and 50, all formulations were positively charged, with a slight reduction of the zeta potential being observed for the HA-lipoplexes, when compared to those of the noncoated lipoplexes (Figure 2). At lower ± ratios, a decrease in zeta potential was observed for all lipoplexes formulations (Figure 2). The shift from positive to negative surface charges for the noncoated liposomes was observed between ± ratios of 2 and 1, which demonstrated that the neutralization of surface charges occurs when there is an equimolarity of positive and negative charges on the lipoplex structure. Interestingly, this turning point from positive to negative surface charge is shifted for the HA-lipoplexes. In this case, the number of siRNA molecules needed to achieve neutrality is smaller, confirming the presence of the negatively charged HA molecules on the liposome structure. The effect of the dilution of HA-liposomes/lipoplexes in physiological media was studied. Both HA-liposomes and HA-lipoplexes (± ratio of 2) maintained their size and surface charge when diluted in 0.9% w/v NaCl and 5% w/v glucose (Figure S1). These data demonstrate previous results confirming that the HA-lipoplexes are rather stable in different media even in the presence of serum.(18)

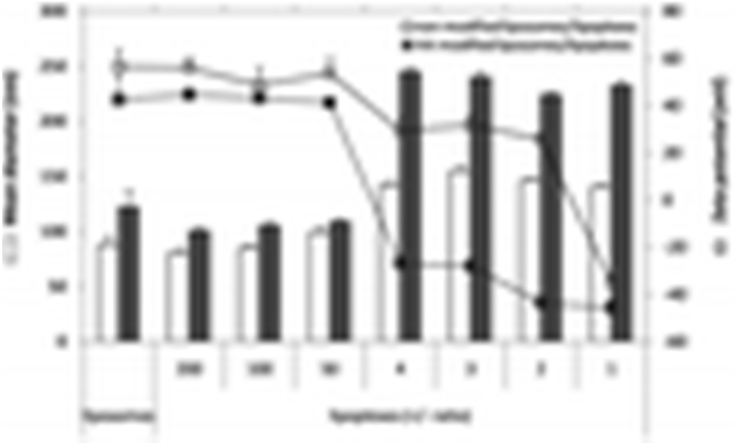

Figure 2. Mean hydrodynamic diameter (bars) and zeta potential (lines) of cationic liposomes and lipoplexes prepared without (gray) or with 10% HA-DOPE (black) at different ± ratios (200, 100, 50, 4, 3, 2, and 1). Data = mean ± SD.

The effect of liposome modification by HA-DOPE on the association rate between liposomes and siRNA to form lipoplexes was measured after the radioactive labeling of siRNA. Interestingly, the presence of HA on the liposome surface did not compromise the association to the siRNA molecules (Figure 3A,B). More than 90% of the added siRNA was bound to the liposomes for ± ratios of as low as 2 (Figure 3 A) while the amount of siRNA bound to lipoplexes increased progressively, reaching approximately 300 μg/mg of lipids (Figure 3B). The maximum entrapment efficiency of nucleotides is commonly described for lipoplex-like structures.(29-32) The strong interactions between the negative phosphate groups on nucleotides and the positive charges of amino groups on cationic lipids lead to such a high association efficiency.(33-35) However, this binding decreased to 60–70% at a ± ratio of 1, indicating a possible saturation of the available positively charged binding sites on the liposomes occurring between ± ratios of 1 and 2 (Figure 3 A). Lipoplexes at ± ratio 2 (negative zeta potential) were chosen for further experiments while in some cases and to understand lipoplex formation higher ± ratios were used (positively charged close to the initial liposome characteristics). Noncoated liposomes and their respective lipoplexes were used for comparison.

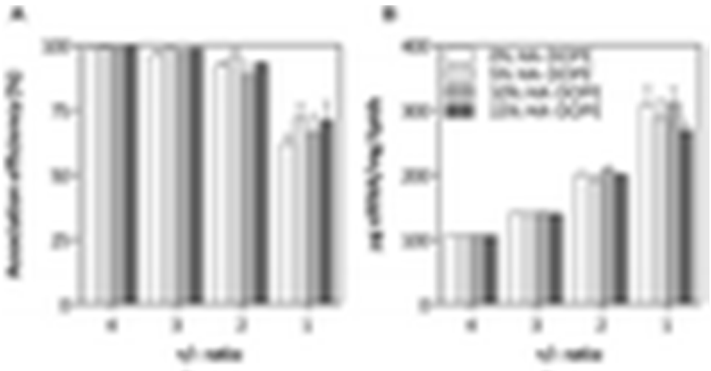

Figure 3. (A) siRNA association efficiency (%) to liposomes and (B) siRNA loading ($\mu g_{siRNA}/mg_{lipids}$) of lipoplexes as a function of the ± ratio and the HA-DOPE content of the parent liposomes. Data = mean ± SD.

The heat exchanged during the interaction between DE/DOPE liposomes and siRNA was analyzed by isothermal titration calorimetry. Figure 4 shows the cumulative heat curves plotted against the siRNA/DE molar ratios for each liposome type, with the raw ITC data processed and fitted to obtain the thermodynamic parameters of the interaction. A first negative enthalpy change occurs in the interaction of both noncoated and HA-liposomes with siRNA molecules. This exothermic reaction represents the interaction between DE lipid molecules and siRNA, and the fact that it occurs almost identically for both samples confirms the previous observation that the presence of HA does not prevent the interaction between siRNA and DE.

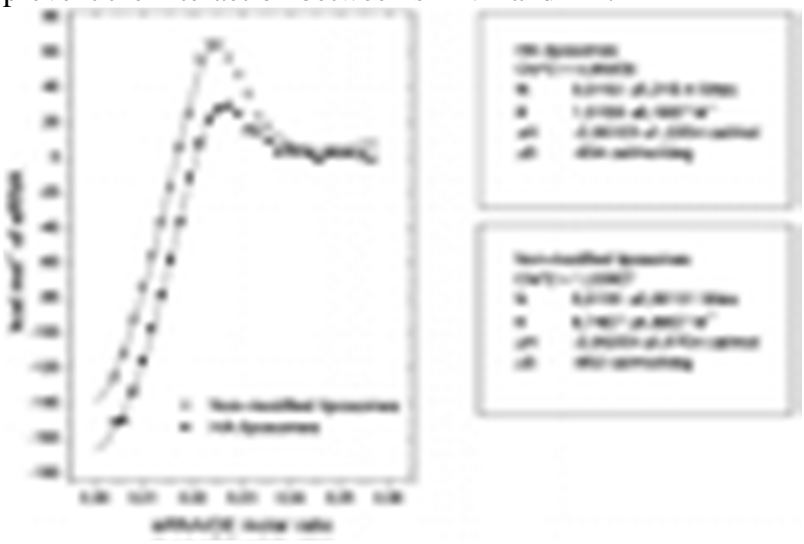

Figure 4. Cumulative heat curves and thermodynamic parameters obtained from the calorimetric titration of siRNA solution at 19.7 μM (10 μL/injection) into noncoated or an HA-liposome suspension at 98 μM.

The exothermic binding of siRNA molecules to liposomes was observed until all of the binding sites in the liposomes were occupied at a ± ratio of 1, corresponding to a molar ratio of siRNA/DE of 0.025, as evidenced by radioactivity measurements. The monotonous decrease in the amount of heat produced after each injection suggested that there is only one type of binding site in the liposomes.(36) These observations are in agreement with reports from the literature on thermodynamic studies of DNA lipoplexes containing DOPE in their composition.(37-39) They are related to the fact that DOPE amine groups (pK_a = 9.5) are unprotonated before binding due to the high surface pH usually measured in cationic liposomes (around 11) whereas proton uptake occurs upon lipoplex formation.(39) Since DOPE protonation is an exothermic process, it is suggested, as

shown in DOTAP/DOPE-containing lipoplex,(37) that changes in the protonation state of DOPE account for the exothermic nature of complex formation with these lipids.
An assessment of the HA-DOPE conjugate purity and a determination of the HA-DOPE fraction bound to liposomes and lipoplexes were carried out by capillary electrophoresis. The HA-DOPE migration time was 5 min, and the electrophoretic profile of the conjugate did not display the characteristic peak of unconjugated HA expected at 8 min, demonstrating the absence of free HA in the conjugate (Figure S2). Large amounts of the HA-DOPE conjugate added to the formulations were found to be associated with the liposomes and lipoplexes at a ± ratio of 134 (66 and 78%, respectively) (Table 1). A decrease in HA-conjugate associated with lipoplexes at a ± ratio of 2, reaching 36%, was observed (Table 1). A similar phenomenon was previously observed for lipoplexes prepared using plasmid DNA.(18) As discussed above, the association of nucleotide molecules to cationic lipids is known to be strong and commonly yields stable lipoplexes with high association efficiencies.(33, 40) We hypothesized that the large and concentrated number of negative charges on the siRNA molecules leads to a competition with the negative charges of HA for interaction with the positive charges of cationic lipids, causing some displacement of HA-DOPE conjugate molecules from the liposome structure. This implies that HA-DOPE insertion into the lipoplexes occurs not only through the DOPE moiety but also via electrostatic interactions.

Table 1. HA-DOPE Conjugate Association Efficiency to Liposomes and Lipoplexes Prepared at ± Ratios of 134 and 2

Preparation	**% HA-DOPE associated**
liposomes DE/DOPE/DOPE-HA	66.5 ± 3.9
lipoplexes DE/DOPE/DOPE-HA/siRNA (±134)	78.8 ± 9.8
lipoplexes DE/DOPE/DOPE-HA/siRNA (±2)	36.3 ± 3.9

Cryo-TEM images of cationic liposomes revealed the coexistence of spherical unilamellar and oligolamellar vesicles (Figure 5). The diameters observed were in the range of the hydrodynamic diameters measured, with some degree of heterogeneity correlated to a measured polydispersity index of 0.22. A modification of this morphology was observed after the addition of siRNA to liposomes. At a ± ratio of 134, the lipoplex shape was less spherical and homogeneous than the liposome shape (Figure 5A,B). At a ± ratio of 2, the structural changes were even more pronounced (Figure 5C). All liposomes/lipoplexes appeared as dense multilamellar structures, suggesting a reorganization of lipids in the presence of siRNA. In particular, the intralamellar distances appeared to be smaller than those observed on the parent oligolamellar liposomes. These observed lipoplexes can be compared to the well-known “sandwich” structures,(29, 41-43) suggesting the presence of electron-dense siRNA molecules intercalated between the cationic lipidic membranes.(6) The deformation and rearrangement of the liposomal membranes are a result of the strong electrostatic interaction between cationic lipid headgroups and siRNA phosphate groups.(29, 43) This structural modification is beneficial as far as siRNA stability is concerned. Indeed, the bilayer packing around each other promotes the protection of the siRNA molecules from degradation better than an exclusive surface association, in which they would be more susceptible to degradation by serum nucleases.(29, 44)

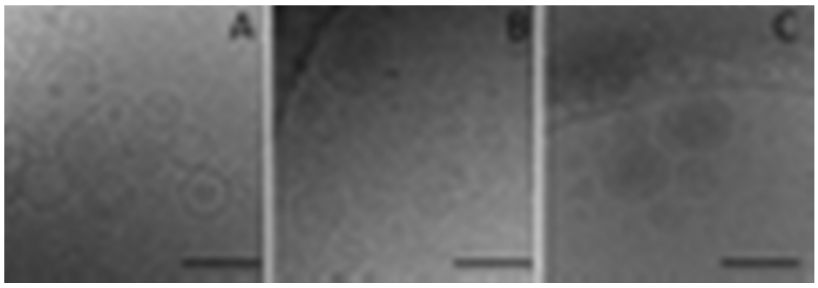

Figure 5. Cryo-TEM images of (A) HA-liposomes, (B) HA-lipoplexes at a ± ratio of 134, and (C) HA-lipoplexes at a ± ratio of 2. Scale bars = 200 nm.

Evidence of the siRNA localization was provided by cryo-TEM analysis. When the particles were submitted to the electron beam for image acquisition, the formation of "bubbles" was observed (Figure 6). Micrographs were recorded at approximately 3 electrons/Å^2 per exposure, with intervals of 10 s between exposures. Bubbling started on the second exposure with the appearance of several small bubbles, which merge to give fewer and larger ones later in the exposure sequence. This occurred for all of the ±2 lipoplexes, a few of the ±134 lipoplexes, and none of the liposomes structures, indicating that this event occurred only when siRNA was present. The pattern of bubble formation inside the vesicles is shown in Figure 6. We hypothesize that bubbling is due to the degradation of water molecules associated with the siRNAs, since the pattern of bubble formation observed is characteristic of the formation of hydrogen gas upon electron radiation of samples.(45, 46) Bubblegram imaging has been previously used for the structural localization of proteins in vitrified specimens and DNA virus internal structure investigation.(47-49) We report here for the first time bubble formation evidencing siRNA localization within the lipoplexes. The uniform localization of the bubbles confirms the distribution of siRNA molecules within the lipoplexes, intercalated with the lipid membranes.

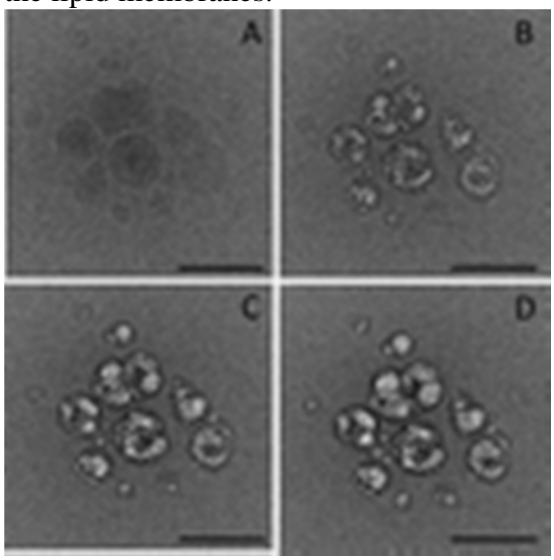

Figure 6. Cryo-TEM images of HA-lipoplexes at a ± ratio of 2 after exposure to approximately (A) 3, (B) 6, (C) 9, and (D) 12 electrons/Å^2, evidencing the formation of bubbles where siRNA is present. Scale bars = 200 nm.

The structure of noncoated and HA-liposomes with 5, 10, and 15% HA-DOPE was further investigated using synchrotron small-angle X-ray scattering (SAXS). The pattern of the noncoated liposome suspension exhibits a broad bump, consistent with the bilayer form factor of unilamellar vesicles(50) (Figure 7A). The SAXS curves of HA-liposomes reveal the gradual increase in the diffraction peak intensities when increasing amounts of HA were added to the formulation, indicating

the formation of increasingly dense multilamellar structures.(51) This interestingly highlighted liposome organization in the presence of hyaluronic acid. In our method of liposome preparation, HA is present at the moment the vesicles are formed. We may therefore assume that a portion of the multiple DOPE units bound to each HA molecule intercalates within the DOPE and DE bilayers upon liposome preparation.(25, 52) The correlation between regularly spaced bilayers gives rise to a Bragg peak. A tiny peak is barely detected in the 5% HA-DOPE liposome curve. As the HA-DOPE content in the formulation increases, the intensity of the Bragg peak increases while its full width at half-maximum decreases, indicative of a greater number of bilayers in vesicles and/or of multilamellar vesicles in the preparation. However, the lack of a second-order peak up to 15% HA-DOPE suggests weakly ordered stacks of bilayers. The characteristic repeat spacing (*d* spacing), corresponding to the sum of the bilayer thickness and water thickness, is deduced from the position of the Bragg peak ($d = 2\pi/q$). A small increase in *d* is observed, from $d = 60.4$ Å ($q = 0.104$ Å^{-1}) to $d = 63.4$ Å ($q = 0.099$ Å^{-1}) when the HA-DOPE amount increases from 10 to 15%, likely reflecting a higher hydration of the lamellar phase and a more important steric repulsion. The structural differences between the noncoated and HA-liposomes could be tentatively related to the differences in net surface charge between bilayers. Indeed, a net surface charge induces electrostatic repulsion between bilayers so that they can swell in excess water. The spontaneous formation of unilamellar vesicles in the DOPE/DE system may be explained by electrostatic repulsion overwhelming van der Waals attraction between bilayers. The addition of HA-DOPE leads to a progressive decrease in the bilayer surface charge and consequently in repulsive forces between bilayers so that a multilamellar structure is formed. Furthermore, negatively charged HA could bridge positively charged lipid bilayers.

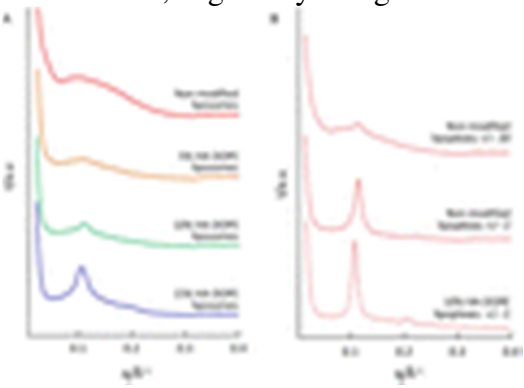

Figure 7. (A) Small-angle X-ray diffraction patterns recorded at room temperature for cationic liposomes, either noncoated or prepared with 5, 10, or 15% HA-DOPE. The gradual increase in the diffraction peak intensity suggests a gradual reorganization of the unilamellar liposomes into oligolamellar structures (a.u = arbitrary units). (B) Small-angle X-ray diffraction patterns recorded at room temperature for noncoated and HA-lipoplexes prepared at ± ratios of 2 and 20. The well-defined Bragg peaks suggest the formation of DOPE/DE-siRNA or HA-DOPE/DE-siRNA complexes, with siRNA confined between regularly stacked lipid bilayers.

As previously reported, siRNA interacts with cationic DOPE/DE liposomes. The SAXS patterns of noncoated lipoplexes evidence the reorganization of unilamellar liposomes into oligolamellar vesicles in the presence of siRNA at low ± ratios. Indeed, at a ±20 ratio, only a small correlation peak appears at $q = 0.116$ Å^{-1} ($d = 54.1$ Å), suggesting that unilamellar liposomes with siRNA absorbed on their surfaces coexist with a few oligolamellar vesicles. In contrast, at a ± ratio of 2, a sharp Bragg peak at $q = 0.112$ Å^{-1} and a faint second order, indicative of a lamellar phase with a *d* spacing of 56.1 Å, are observed (Figure 7B). When HA-liposomes are used for the preparation of lipoplexes (± 2 ratio), a sharper Bragg peak at $q = 0.102$ Å^{-1} and a stronger second order are observed, reflecting a more ordered lamellar phase with a *d* spacing of 61.4 Å. This suggests that siRNA is confined between ordered lipid bilayers. Similar behavior was observed for HA-lipoplexes. These findings are consistent with the existing schematic models of lipoplex formation(42, 53) and with the evolution

of nanoparticle size upon complexation. This gradual modification of vesicle morphology after interaction between siRNA and cationic liposomes measured by SAXS was confirmed by cryo-TEM microscopy as shown above.

The binding affinity to CD44 receptors of noncoated and 10% HA-lipoplexes prepared at a ± ratio of 2 was determined using surface plasmon resonance (SPR). CD44-Fc was immobilized in a stable and suitably oriented manner on the surface, as confirmed by an analysis of the interaction of the receptors with HA solution. HA did not show any binding when exposed to the reference surface, indicating that binding to the receptors was specific. The immobilization protocol allowed the binding of 100–150 RU, corresponding to 0.1–0.15 ng·mm^{-2} of CD44-Fc per channel. Sensorgrams obtained by the interaction of different concentrations of HA-lipoplexes and plain lipoplexes with the CD44-Fc-immobilized sensor chip were used to analyze the binding affinity. Representative sensorgrams obtained in this experiment are shown in Figure 8. Signals of HA-lipoplexes were normalized using signals from nonmodified lipoplexes at the same concentrations to eliminate nonspecific interaction signals. Considering the molecular weight of the CD44-Fc used for these experiments (48.6 kDa), we estimate that 12.3–18.5 receptors were immobilized per nm^2. The difference between the obtained signals reveals a concentration-dependent and preferential affinity of HA-lipoplexes compared to the nonmodified lipoplexes (Figure 8), thereby confirming both the suitable positioning of HA on the lipoplex surface and the HA ability to bind specifically to the CD44 receptors. The CD44-Fc immobilization combined with the surface rinsing protocol after HA interactions represents a significant improvement in the SPR techniques to analyze HA binding to CD44. First, the low sensor surface capacity was suitable for the interaction studies.(54) Previously reported SPR data on the HA-CD44 interaction are based on interaction studies on highly loaded sensor surfaces,(55-57) which complicates data analysis and may misrepresent the interaction between HA and CD44.(58) Second, the rinsing protocol promoted the detachment of HA-lipoplexes from the CD44-Fc surface after each analysis without damaging the receptors. This was an experimental hurdle due to the multivalent aspect of this interaction and required many optimization steps. Little or no desorption upon rinsing high-molecular-weight HA molecules after interaction with its receptors has been described until now.(58, 59) The kinetic model that best fit the data obtained was the heterogeneity model with four independent binding sites. Nevertheless, we believe that due to the presence of multiple binding sites on each HA, the complexity of the HA-lipoplex structure, and rebinding events during dissociation, a precise kinetic characterization of the HA-lipoplex–CD44 interaction cannot be properly resolved.

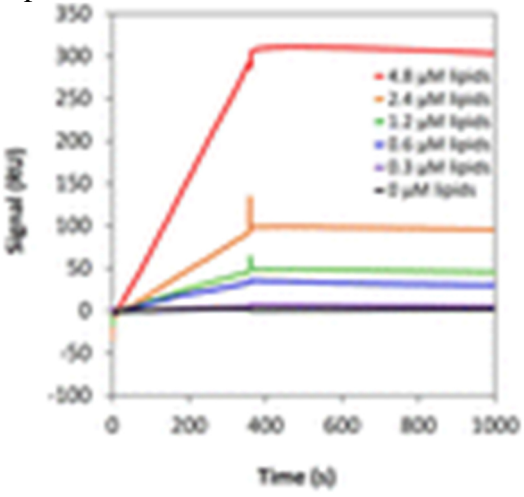

Figure 8. SPR sensorgrams obtained by the injection of 10% HA-lipoplexes ± ratio 2 on CD44-Fc-immobilized sensor chips. Samples were diluted in 150 mM NaCl to 4.8, 2.4, 1.2, 0.6, and 0.3 μM lipids. Signals of HA-lipoplexes were normalized using signals from nonmodified lipoplexes at the same concentrations to eliminate nonspecific interaction signals.

Conclusions

Lipoplexes are promising siRNA delivery systems that have been studied for gene expression inhibition. An accurate and detailed comprehension of their structure and physicochemical characteristics is crucial because of their influence in vitro and in vivo on the efficiency of these nanocarriers. Here, we developed and investigated in detail the structure of novel HA-lipoplexes for the delivery of siRNA. With the combination of radioactive labeling, diameter and surface charge analyses, capillary electrophoresis, cryo-TEM microscopy, SAXS, and surface plasmon resonance, the influence of the components of the formulation on lipoplex morphology was determined. We demonstrated an improvement in the SPR method for CD44-HA binding studies and described for the first time evidence of siRNA localization using cryo-TEM microscopy. We provided additional information showing the interest of lipoplexes containing the HA-DOPE conjugate, which associated large amounts of siRNA, improved stability in physiological media, and provided increasing affinity to CD44 receptors with increasing HA content. These outputs contribute to the improvement of the siRNA lipoplex development and characterization methods and provide future research directions for the characterization of these nanocarriers for successful use in gene delivery.

Acknowledgment

Institut Galien Paris-Sud is a member of the Laboratory of Excellence LERMIT supported by a grant from ANR (ANR-10-LABX-33). This work was financially supported by CAPES, Brazil (process number 5641-10-1). We are grateful for the guidance and assistance of Hélène Chacun (Institut Galien Paris-Sud) with radioactivity experiments.

References

1. Nascimento, T.; Hillaireau, H.; Fattal, E.Nanoscale particles for lung delivery of siRNA J. Drug Delivery Sci. Technol. 2012, 22 (1) 99– 108, DOI: 10.1016/S1773-2247(12)50010-9
2. Soutschek, J.; Akinc, A.; Bramlage, B.; Charisse, K.; Constien, R.; Donoghue, M.; Elbashir, S.; Geick, A.; Hadwiger, P.; Harborth, J.; John, M.; Kesavan, V.; Lavine, G.; Pandey, R. K.; Racie, T.; Rajeev, K. G.; Rohl, I.; Toudjarska, I.; Wang, G.; Wuschko, S.; Bumcrot, D.; Koteliansky, V.; Limmer, S.; Manoharan, M.; Vornlocher, H. P.Therapeutic silencing of an endogenous gene by systemic administration of modified siRNAs Nature 2004, 432 (7014) 173– 8, DOI: 10.1038/nature03121
3. Aagaard, L.; Rossi, J. J.RNAi therapeutics: Principles, prospects and challenges Adv. Drug Delivery Rev. 2007, 59 (2–3) 75– 86, DOI: 10.1016/j.addr.2007.03.005
4. Oh, Y.-K.; Park, T. G.siRNA delivery systems for cancer treatment Adv. Drug Delivery Rev. 2009, 61 (10) 850– 862, DOI: 10.1016/j.addr.2009.04.018
5. Barros, S. A.; Gollob, J. A.Safety profile of RNAi nanomedicines Adv. Drug Delivery Rev. 2012, 64 (15) 1730– 1737, DOI: 10.1016/j.addr.2012.06.007
6. Belletti, D.; Tonelli, M.; Forni, F.; Tosi, G.; Vandelli, M. A.; Ruozi, B.AFM and TEM characterization of siRNAs lipoplexes: A combinatory tools to predict the efficacy of complexation Colloids Surf., A 2013, 436, 459– 466, DOI: 10.1016/j.colsurfa.2013.07.021
7. Kanasty, R. L.; Whitehead, K. A.; Vegas, A. J.; Anderson, D. G.Action and Reaction: The Biological Response to siRNA and Its Delivery Vehicles Mol. Ther. 2012, 20 (3) 513– 524, DOI: 10.1038/mt.2011.294

8. Gershon, H.; Ghirlando, R.; Guttman, S. B.; Minsky, A.Mode of formation and structural features of DNA-cationic liposome complexes used for transfection Biochemistry 1993, 32 (28) 7143– 7151, DOI: 10.1021/bi00079a011
9. Parvizi, P.; Jubeli, E.; Raju, L.; Khalique, N. A.; Almeer, A.; Allam, H.; Manaa, M. A.; Larsen, H.; Nicholson, D.; Pungente, M. D.; Fyles, T. M.Aspects of nonviral gene therapy: Correlation of molecular parameters with lipoplex structure and transfection efficacy in pyridinium-based cationic lipids Int. J. Pharm. 2014, 461 (1–2) 145– 156, DOI: 10.1016/j.ijpharm.2013.11.045
10. Putnam, D.Polymers for gene delivery across length scales Nat. Mater. 2006, 5 (6) 439– 451, DOI: 10.1038/nmat1645
11. Ma, B.; Zhang, S.; Jiang, H.; Zhao, B.; Lv, H.Lipoplex morphologies and their influences on transfection efficiency in gene delivery J. Controlled Release 2007, 123 (3) 184– 194, DOI: 10.1016/j.jconrel.2007.08.022
12. Gratton, S. E.; Ropp, P. A.; Pohlhaus, P. D.; Luft, J. C.; Madden, V. J.; Napier, M. E.; DeSimone, J. M.The effect of particle design on cellular internalization pathways Proc. Natl. Acad. Sci. U. S. A. 2008, 105 (33) 11613– 11618, DOI: 10.1073/pnas.0801763105
13. Mahato, R. I.Water insoluble and soluble lipids for gene delivery Adv. Drug Delivery Rev. 2005, 57 (5) 699– 712, DOI: 10.1016/j.addr.2004.12.005
14. Arpicco, S.; De Rosa, G.; Fattal, E.Lipid-based nanovectors for targeting of CD44-overexpressing tumor cells J. Drug Delivery 2013, 2013, 1, DOI: 10.1155/2013/860780
15. Laurent, T. C.; Fraser, J.Hyaluronan FASEB J. 1992, 6 (7) 2397– 2404
16. Noble, P. W.Hyaluronan and its catabolic products in tissue injury and repair Matrix Biol. 2002, 21 (1) 25– 9, DOI: 10.1016/S0945-053X(01)00184-6
17. Deed, R.; Rooney, P.; Kumar, P.; Norton, J. D.; Smith, J.; Freemont, A. J.; Kumar, S.Early-response gene signalling is induced by angiogenic oligosaccharides of hyaluronan in endothelial cells. Inhibition by non-angiogenic, high-molecular-weight hyaluronan Int. J. Cancer 1997, 71 (2) 251– 6, DOI: 10.1002/(SICI)1097-0215(19970410)71:2<251::AID-IJC21>3.0.CO;2-J
18. Wojcicki, A. D.; Hillaireau, H.; Nascimento, T. L.; Arpicco, S.; Taverna, M.; Ribes, S.; Bourge, M.; Nicolas, V.; Bochot, A.; Vauthier, C.Hyaluronic acid-bearing lipoplexes: physico-chemical characterization and in vitro targeting of the CD44 receptor J. Controlled Release 2012, 162, 545, DOI: 10.1016/j.jconrel.2012.07.015
19. Eliaz, R. E.; Szoka, F. C., Jr.Liposome-encapsulated doxorubicin targeted to CD44: a strategy to kill CD44-overexpressing tumor cells Cancer Res. 2001, 61 (6) 2592– 601
20. Peer, D.; Florentin, A.; Margalit, R.Hyaluronan is a key component in cryoprotection and formulation of targeted unilamellar liposomes Biochim. Biophys. Acta, Biomembr. 2003, 1612 (1) 76– 82, DOI: 10.1016/S0005-2736(03)00106-8
21. Peer, D.; Margalit, R.Loading mitomycin C inside long circulating hyaluronan targeted nano-liposomes increases its antitumor activity in three mice tumor models Int. J. Cancer 2004, 108 (5) 780– 9, DOI: 10.1002/ijc.11615
22. Qhattal, H. S. S.; Liu, X.Characterization of CD44-Mediated Cancer Cell Uptake and Intracellular Distribution of Hyaluronan-Grafted Liposomes Mol. Pharmaceutics 2011, 8 (4) 1233– 1246, DOI: 10.1021/mp2000428
23. Arpicco, S.; Canevari, S.; Ceruti, M.; Galmozzi, E.; Rocco, F.; Cattel, L.Synthesis, characterization and transfection activity of new saturated and unsaturated cationic lipids Farmaco 2004, 59 (11) 869– 78, DOI: 10.1016/j.farmac.2004.06.007
24. Taetz, S.; Bochot, A.; Surace, C.; Arpicco, S.; Renoir, J. M.; Schaefer, U. F.; Marsaud, V.; Kerdine-Roemer, S.; Lehr, C. M.; Fattal, E.Hyaluronic Acid-Modified DOTAP/DOPE Liposomes for the Targeted Delivery of Anti-Telomerase siRNA to CD44-Expressing Lung Cancer Cells Oligonucleotides 2009, 19 (2) 103– 115, DOI: 10.1089/oli.2008.0168

25. Surace, C.; Arpicco, S.; Dufay-Wojcicki, A.; Marsaud, V.; Bouclier, C.; Clay, D.; Cattel, L.; Renoir, J. M.; Fattal, E.Lipoplexes Targeting the CD44 Hyaluronic Acid Receptor for Efficient Transfection of Breast Cancer Cells Mol. Pharmaceutics 2009, 6 (4) 1062– 1073, DOI: 10.1021/mp800215d
26. Batzri, S.; Korn, E. D.Single bilayer liposomes prepared without sonication Biochim. Biophys. Acta, Biomembr. 1973, 298, 1015– 1019, DOI: 10.1016/0005-2736(73)90408-2
27. Grimshaw, J.; Trocha-Grimshaw, J.; Fisher, W.; Rice, A.; Smith, S.; Spedding, P.; Duffy, J.; Mollan, R.Quantitative analysis of hyaluronan in human synovial fluid using capillary electrophoresis Electrophoresis 1996, 17 (2) 396– 400, DOI: 10.1002/elps.1150170218
28. Stewart, J. C. M.Colorimetric determination of phospholipids with ammonium ferrothiocyanate Anal. Biochem. 1980, 104 (1) 10– 14, DOI: 10.1016/0003-2697(80)90269-9
29. Li, W.; Szoka, F. C., JrLipid-based nanoparticles for nucleic acid delivery Pharm. Res. 2007, 24 (3) 438– 449, DOI: 10.1007/s11095-006-9180-5
30. Kesharwani, P.; Gajbhiye, V.; Jain, N. K.A review of nanocarriers for the delivery of small interfering RNA Biomaterials 2012, 33 (29) 7138– 7150, DOI: 10.1016/j.biomaterials.2012.06.068
31. Wu, S. Y.; Putral, L. N.; Liang, M.; Chang, H.-I.; Davies, N. M.; McMillan, N. A.Development of a novel method for formulating stable siRNA-loaded lipid particles for in vivo use Pharm. Res. 2009, 26 (3) 512– 522, DOI: 10.1007/s11095-008-9766-1
32. Kapoor, M.; Burgess, D. J.Efficient and safe delivery of siRNA using anionic lipids: formulation optimization studies Int. J. Pharm. 2012, 432 (1) 80– 90, DOI: 10.1016/j.ijpharm.2012.04.058
33. Lu, H.-D.; Zhao, H.-Q.; Wang, K.; Lv, L.-L.Novel hyaluronic acid–chitosan nanoparticles as non-viral gene delivery vectors targeting osteoarthritis Int. J. Pharm. 2011, 420 (2) 358– 365, DOI: 10.1016/j.ijpharm.2011.08.046
34. Kim, A. J.; Boylan, N. J.; Suk, J. S.; Lai, S. K.; Hanes, J.Non-degradative intracellular trafficking of highly compacted polymeric DNA nanoparticles J. Controlled Release 2012, 158 (1) 102– 107, DOI: 10.1016/j.jconrel.2011.10.031
35. Landesman-Milo, D.; Goldsmith, M.; Leviatan Ben-Arye, S.; Witenberg, B.; Brown, E.; Leibovitch, S.; Azriel, S.; Tabak, S.; Morad, V.; Peer, D.Hyaluronan grafted lipid-based nanoparticles as RNAi carriers for cancer cells Cancer Lett. 2013, 334 (2) 221– 227, DOI: 10.1016/j.canlet.2012.08.024
36. Ikonen, M.; Murtomäki, L.; Kontturi, K.Microcalorimetric and zeta potential study on binding of drugs on liposomes Colloids Surf., B 2010, 78 (2) 275– 282, DOI: 10.1016/j.colsurfb.2010.03.017
37. Pozharski, E.; MacDonald, R. C.Thermodynamics of Cationic Lipid-DNA Complex Formation as Studied by Isothermal Titration Calorimetry Biophys. J. 2002, 83 (1) 556– 565, DOI: 10.1016/S0006-3495(02)75191-6
38. Gonçalves, E.; Debs, R. J.; Heath, T. D.The effect of liposome size on the final lipid/DNA ratio of cationic lipoplexes Biophys. J. 2004, 86 (3) 1554– 1563, DOI: 10.1016/S0006-3495(04)74223-X
39. Lobo, B. A.; Koe, G. S.; Koe, J. G.; Middaugh, C. R.Thermodynamic analysis of binding and protonation in DOTAP/DOPE (1:1): DNA complexes using isothermal titration calorimetry Biophys. Chem. 2003, 104 (1) 67– 78, DOI: 10.1016/S0301-4622(02)00339-3
40. De Rosa, G.; De Stefano, D.; Laguardia, V.; Arpicco, S.; Simeon, V.; Carnuccio, R.; Fattal, E.Novel cationic liposome formulation for the delivery of an oligonucleotide decoy to NF-kappaB into activated macrophages Eur. J. Pharm. Biopharm. 2008, 70 (1) 7– 18, DOI: 10.1016/j.ejpb.2008.03.012

41. Gustafsson, J.; Arvidson, G.; Karlsson, G.; Almgren, M.Complexes between cationic liposomes and DNA visualized by cryo-TEM Biochim. Biophys. Acta, Biomembr. 1995, 1235 (2) 305– 312, DOI: 10.1016/0005-2736(95)80018-B
42. Huebner, S.; Battersby, B. J.; Grimm, R.; Cevc, G.Lipid-DNA complex formation: reorganization and rupture of lipid vesicles in the presence of DNA as observed by cryoelectron microscopy Biophys. J. 1999, 76 (6) 3158– 66, DOI: 10.1016/S0006-3495(99)77467-9
43. Xu, Y.; Hui, S.-W.; Frederik, P.; Szoka, F. C., JrPhysicochemical characterization and purification of cationic lipoplexes Biophys. J. 1999, 77 (1) 341– 353, DOI: 10.1016/S0006-3495(99)76894-3
44. Peer, D.; Lieberman, J.Special delivery: targeted therapy with small RNAs Gene Ther. 2011, 18 (12) 1127– 1133, DOI: 10.1038/gt.2011.56
45. Leapman, R. D.; Sun, S.Cryo-electron energy loss spectroscopy: observations on vitrified hydrated specimens and radiation damage Ultramicroscopy 1995, 59 (1) 71– 79, DOI: 10.1016/0304-3991(95)00019-W
46. Meents, A.; Gutmann, S.; Wagner, A.; Schulze-Briese, C.Origin and temperature dependence of radiation damage in biological samples at cryogenic temperatures Proc. Natl. Acad. Sci. U. S. A. 2010, 107 (3) 1094– 1099, DOI: 10.1073/pnas.0905481107
47. Black, L. W.; Thomas, J. A. Condensed Genome Structure. In Viral Molecular Machines; Springer, 2012; pp 469– 487.
48. Wu, W.; Thomas, J. A.; Cheng, N.; Black, L. W.; Steven, A. C.Bubblegrams reveal the inner body of bacteriophage ϕKZ Science 2012, 335 (6065) 182– 182, DOI: 10.1126/science.1214120
49. Cheng, N.; Wu, W.; Watts, N. R.; Steven, A. C.Exploiting radiation damage to map proteins in nucleoprotein complexes: The internal structure of bacteriophage T7 J. Struct. Biol. 2014, 185 (3) 250– 256, DOI: 10.1016/j.jsb.2013.12.004
50. Bouwstra, J. A.; Gooris, G. S.; Bras, W.; Talsma, H.Small-angle X-ray-scattering - Possibilities and limitations in characterization of vesicles Chem. Phys. Lipids 1993, 64 (1– 3) 83– 98, DOI: 10.1016/0009-3084(93)90059-C
51. Battersby, B. J.; Grimm, R.; Huebner, S.; Cevc, G.Evidence for three-dimensional interlayer correlations in cationic lipid-DNA complexes as observed by cryo-electron microscopy Biochim. Biophys. Acta, Biomembr. 1998, 1372 (2) 379– 383, DOI: 10.1016/S0005-2736(98)00062-5
52. Arpicco, S.; Lerda, C.; Dalla Pozza, E.; Costanzo, C.; Tsapis, N.; Stella, B.; Donadelli, M.; Dando, I.; Fattal, E.; Cattel, L.Hyaluronic acid-coated liposomes for active targeting of gemcitabine Eur. J. Pharm. Biopharm. 2013, 85 (3) 373– 380, DOI: 10.1016/j.ejpb.2013.06.003
53. Weisman, S.; Hirsch-Lerner, D.; Barenholz, Y.; Talmon, Y.Nanostructure of cationic lipid-oligonucleotide complexes Biophys. J. 2004, 87 (1) 609– 614, DOI: 10.1529/biophysj.103.033480
54. Myszka, D. G.Improving biosensor analysis J. Mol. Recognit. 1999, 12 (5) 279– 284, DOI: 10.1002/(SICI)1099-1352(199909/10)12:5<279::AID-JMR473>3.0.CO;2-3
55. Ogino, S.; Nishida, N.; Umemoto, R.; Suzuki, M.; Takeda, M.; Terasawa, H.; Kitayama, J.; Matsumoto, M.; Hayasaka, H.; Miyasaka, M.Two-state conformations in the hyaluronan-binding domain regulate CD44 adhesiveness under flow condition Structure 2010, 18 (5) 649– 656, DOI: 10.1016/j.str.2010.02.010
56. Sebban, L. E.; Ronen, D.; Levartovsky, D.; Elkayam, O.; Caspi, D.; Aamar, S.; Amital, H.; Rubinow, A.; Golan, I.; Naor, D.The involvement of CD44 and its novel ligand galectin-8 in apoptotic regulation of autoimmune inflammation J. Immunol. 2007, 179 (2) 1225– 1235, DOI: 10.4049/jimmunol.179.2.1225

57. Banerji, S.; Hide, B. R.; James, J. R.; Noble, M. E.; Jackson, D. G.Distinctive properties of the hyaluronan-binding domain in the lymphatic endothelial receptor Lyve-1 and their implications for receptor function J. Biol. Chem. 2010, 285 (14) 10724– 10735, DOI: 10.1074/jbc.M109.047647
58. Mizrahy, S.; Raz, S. R.; Hasgaard, M.; Liu, H.; Soffer-Tsur, N.; Cohen, K.; Dvash, R.; Landsman-Milo, D.; Bremer, M. G. E. G.; Moghimi, S. M.Hyaluronan-coated nanoparticles: The influence of the molecular weight on CD44-hyaluronan interactions and on the immune response J. Controlled Release 2011, 156 (2) 231– 238, DOI: 10.1016/j.jconrel.2011.06.031
59. Wolny, P. M.; Banerji, S.; Gounou, C.; Brisson, A. R.; Day, A. J.; Jackson, D. G.; Richter,R. P.Analysis of cd44-hyaluronan interactions in an artificial membrane system insights into the distinct binding properties of high and low molecular weight hyaluronan J. Biol. Chem. 2010, 285 (39) 30170– 30180, DOI: 10.1074/jbc.M110.137562

Nascimento et al. Supramolecular organization and siRNA binding of hyaluronic acid-coated lipoplexes for targeted delivery to CD44 receptor

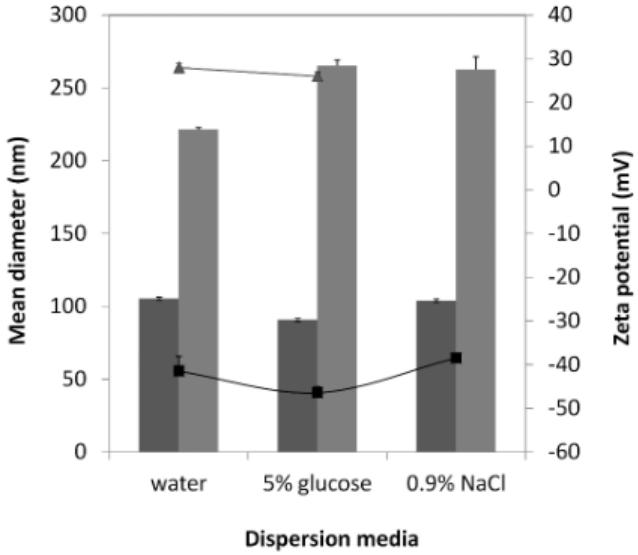

Figure S1. Mean hydrodynamic diameter (bars) and zeta potential (lines) of HA-modified liposomes (gray) and lipoplexes (black) +/– ratio 2 diluted in water, 5% w/v glucose or 0.9% w/v NaCl. Data = mean ± SD.